Supporting Information for:

Metallurgical approach to enhance electrochemical activities of magnesium anodes for magnesium rechargeable batteries

Toshihiko Mandai,[†,*] *and Hidetoshi Somekawa*[‡]

[†]Center for Research on Energy and Environmental Materials, National Institute for Materials Science, 1-1 Namiki, Ibaraki, 305-0044 Japan.

[‡]Research Center for Structural Materials, National Institute for Materials Science, 1-2-1 Sengen, Ibaraki, 305-0047 Japan.

CORRESPONDING AUTHOR FOOTNOTES

Telephone: +81-29-860-4464, E-mail: MANDAI.Toshihiko@nims.go.jp

Experimental details, a list of overpotential observed for Mg-X alloys (Table S1), cyclic voltammograms (CVs) of magnesium single crystals (Fig. S1) and commercial magnesium ribbon (Fig. S2), HAADF-STEM images of a series of Mg-X (Fig. S3), CVs of Mg-X cycled in a typical Grignard reagent (Fig. S4), SEM images of the selected Mg-X after CV cycling (Fig. S5), Coulombic efficiency for deposition/dissolution (Fig. S6) and full-cell cycling (Fig. S7) were given. The EBSD mapping of magnesium samples were also displayed in the corresponding figures (Fig. S1 and S2).

Experimental details

Magnesium anode preparation

Mg single crystals with different orientation ((0001) and (1010); from MaTecK, commercial purity grade of 99.999%), pure Mg (pMg; commercial purity grade of 99.96 %) and several Mg-0.3at.% X (X = Ag, Al, Bi, Ca, Li, Mn, Pb, Sn, Y and Zn) binary alloys were used. These alloying elements have a maximum solubility of more than 0.3 at% in Mg. The alloying amount of 0.3 at% was applied in this study (i) to prevent large-sized precipitation, (ii) to investigate alloying effect using many typed Mg binary alloys and (iii) to make easy preparation as for measuring weights. The binary alloys were prepared by casting, followed by solution treatments at temperature of 773 K for 24 hours under CO_2 atmosphere. These solution treated Mg-X and pMg were extruded at 423 to 623 K with extrusion ratio of 32. The shape of extrusion bar had a thickness of 2 mm, width of 30 mm and length of more than 1,000 mm. The extruded Mg-X and pMg were annealed to control grain size of approximately 30 μm at various temperatures of 523 to 623 up to 10 hours. The Mg-X and pMg bars were cut into strips with their geometries of 5 × 50 × 0.2 mm. The strips were covered with a kapton tape, followed by peeled the tape off with 2 mm diameter to expose the fixed area of pMg and Mg-X. Prior to the electrochemical measurements, the exposed area was mechanically polished with emery papers #400, #2400, and #4000, then the strips were washed with anhydrous THF to remove turnings.

Electrolyte Preparation

Di-*n*-butyl magnesium ($Mg(Bu)_2$; 1.0 mol dm^{-3} heptane solution) was purchased from Sigma-Aldrich and used as received. Tetrahydrofuran-borane tetrahydrofuran solution (BH_3-THF) and 1,1,1,3,3,3-Hexafluoroisopropanol (HFIP-H) were purchased from FUJIFILM Wako Chemicals. HFIP-H was distilled over calcium oxide and stored in an Ar-filled glovebox with 3A molecular sieves. Diglyme (G2) for electrochemistry was obtained from Kanto Chemical Co., Inc., and used without further purification. A typical Grignard reagent, *ca*. 2 mol dm^{-3} C_2H_5MgCl/THF was purchased from Tokyo Chemical Industry CO., Ltd., and used as received.

$Mg[B(HFIP)_4]_2$ was synthesized according to the procedure described elsewhere.[1] The electrolyte solution of 0.3 mol dm^{-3} $Mg[B(HFIP)_4]_2$/G2 was prepared by dissolving the prefixed amounts of $Mg[B(HFIP)_4]_2$ into G2, followed by vigorous stirring at 30 °C overnight in the glovebox (< 1 ppm H_2O and O_2). The water content of the prepared electrolytes measured by Karl Fischer titration was confirmed as less than 50 ppm.

Measurements

The grain size and crystal orientation of pMg and Mg-X were characterized by electron back scattered diffraction pattern (EBSD) mapping. The HAADF-STEM images of a series of Mg-X were obtained by using JEM-ARM200F (JEOL). The Mg-X samples were processed by a focused ion beam to obtain a smooth surface view. The elemental analysis was subsequently carried out on the same sample by energy dispersive X-ray spectroscopy (EDX) and electron energy loss spectroscopy (EELS).

Cyclic voltammetry was performed using a typical three-electrode cell by an electrochemical analyzer (HSV-110, Hokuto). A mechanically polished pMg and Mg-X (0.2 mm diameter) was served as a working electrode. A coiled Pt wire was employed as a counter electrode. A Ag^{+}/Ag reference electrode was fabricated according to a procedure described elsewhere.[2] The Mg^{2+}/Mg^{0} potential in the 0.3 mol dm^{-3} $Mg[B(HFIP)_4]_2$/G2 and *ca*. 2 mol dm^{-3} C_2H_5MgCl/THF electrolytes were calibrated to be −2.49 V and 2.62 V *vs*. the reference, respectively.[1,2] Galvanostatic magnesium dissolution/deposition cycling tests were carried out using a symmetric two-electrode assemblies with an automatic charge/discharge instrument (HJ0610SD8Y, Hokuto Denko). A current density of 0.5 mA cm^{-2} for 30 min for each dissolution and deposition at 30 °C was adopted. A galvanostatic discharge-charge cycling was performed on the [$MgMn_2O_4$ | 0.3 mol dm^{-3} $Mg[B(HFIP)_4]_2$/G2 | Mg-X] cells. The cycling test was carried out in the voltage range of 0.2–4.0 V at 30 ºC with a current density of 10.4 mA g^{-1} (at C/25-rate based on the mass of $MgMn_2O_4$). The $MgMn_2O_4$ cathode was prepared by mixing $MgMn_2O_4$ powder as a cathode active material, acetylene black as a conducting agent, and PTFE as a binder, according to the reported procedure.[3]

Table S1. A list of the overpotential (η) observed for the initial anodic process of pMg and Mg-X alloys. The overpotential was defined as the potential where a current density of ±0.1 mA cm^{-2} was observed.

Samples	η / mV	$\Delta\eta$ (= $\eta_{Mg\text{-}X} - \eta_{pMg}$)
pMg	140	
Mg-Ag	260	120
Mg-Al	240	100
Mg-Bi	240	100
Mg-Ca	230	90
Mg-Li	220	80
Mg-Mn	220	80
Mg-Sn	240	100
Mg-Y	180	40
Mg-Zn	250	110

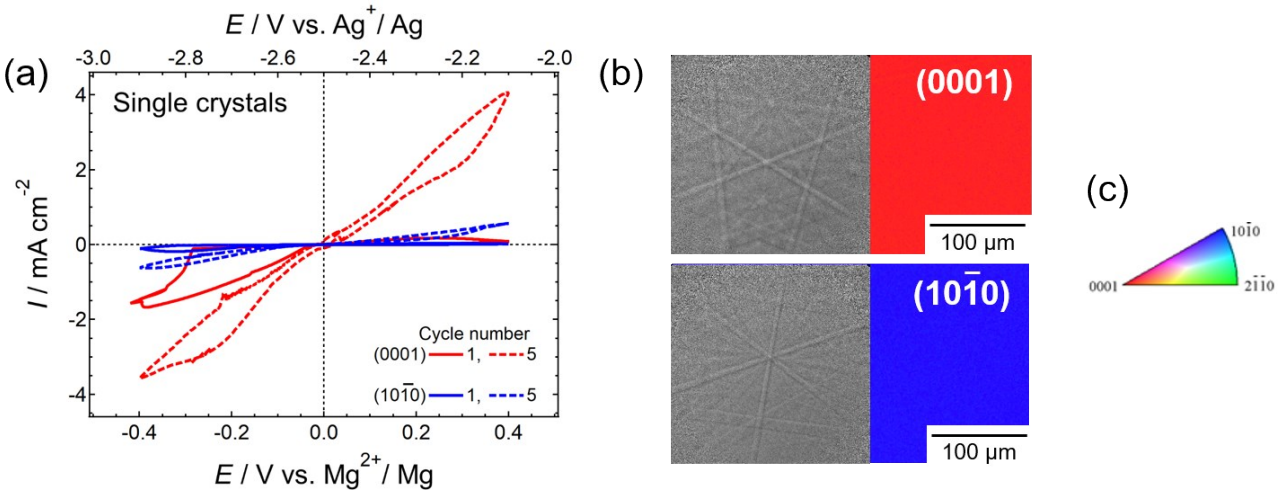

Figure S1. (a) Cyclic voltammograms (CVs) of the single crystals of magnesium recorded in 0.3 mol dm^{-3} $Mg[B(HFIP)_4]_2$/G2 at scan rate of 10 mV s^{-1} and at 30 °C. (b) EBSD mapping and Kikuchi patterns of the single crystals tested here. (c) A color indicator for mirror indices.

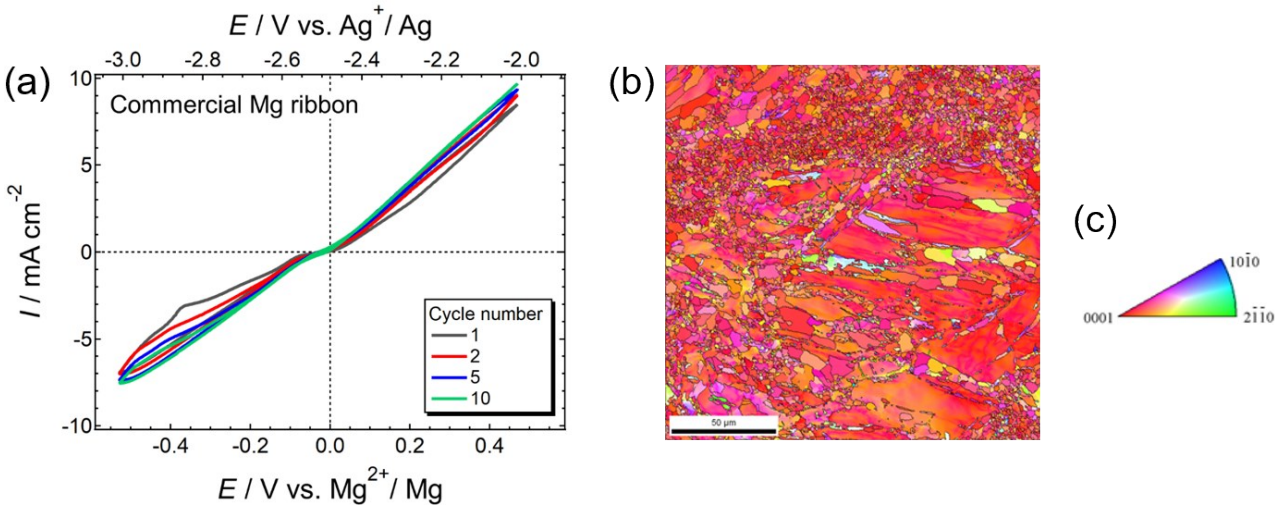

Figure S2. (a) CVs of the commercial magnesium ribbon recorded in 0.3 mol dm^{-3} $Mg[B(HFIP)_4]_2$/G2 at scan rate of 10 mV s^{-1} and at 30 °C. (b) EBSD mapping of the sample. (c) A color indicator for mirror indices.

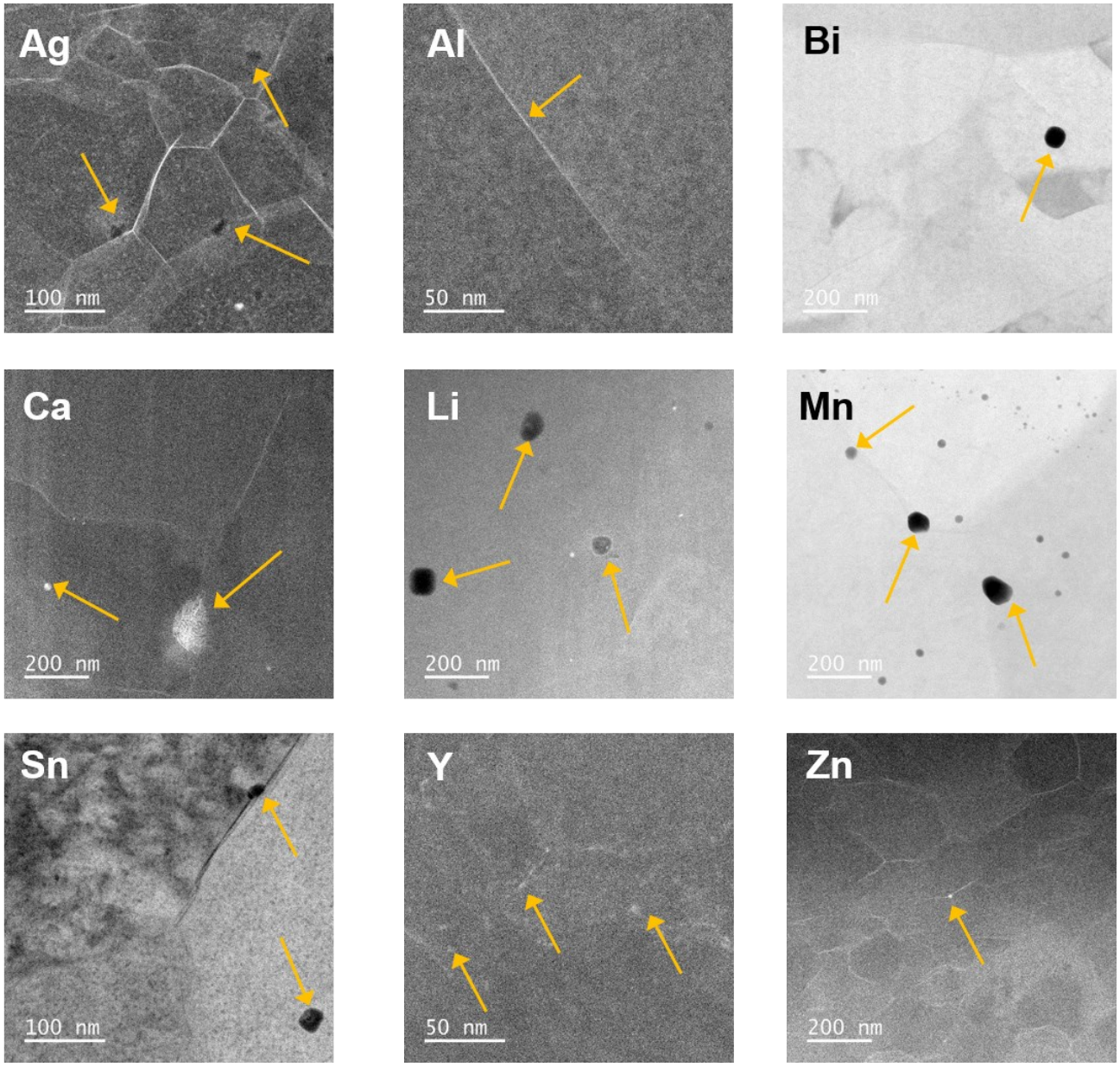

Figure S3. HAADF-STEM images of a series of Mg-X. To highlight the segregation behavior of alloying elements, bright and dark fields were selected depending the samples. Yellow arrows in the images point the alloying elements.

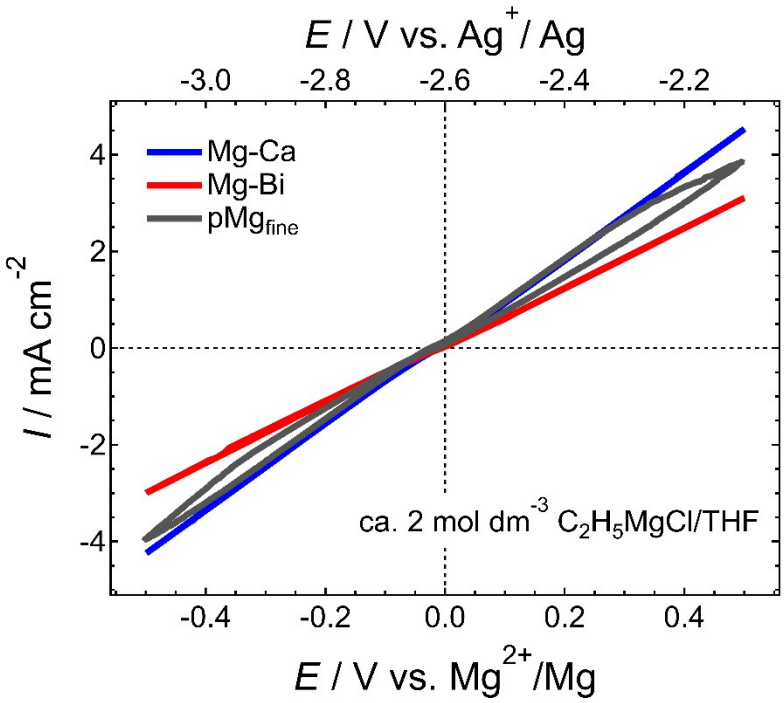

Figure S4. 10th cycle CV curves of pMg_{fine}, Mg-Ca, and Mg-Bi cycled in ca. 2 mol dm^{-3} C_2H_5MgCl/THF at 30 °C. CV measurements were conducted using a three-electrode cell, where pMg or Mg-X, Pt coil, and Ag^+/Ag were served as working, counter, and reference electrodes, respectively.

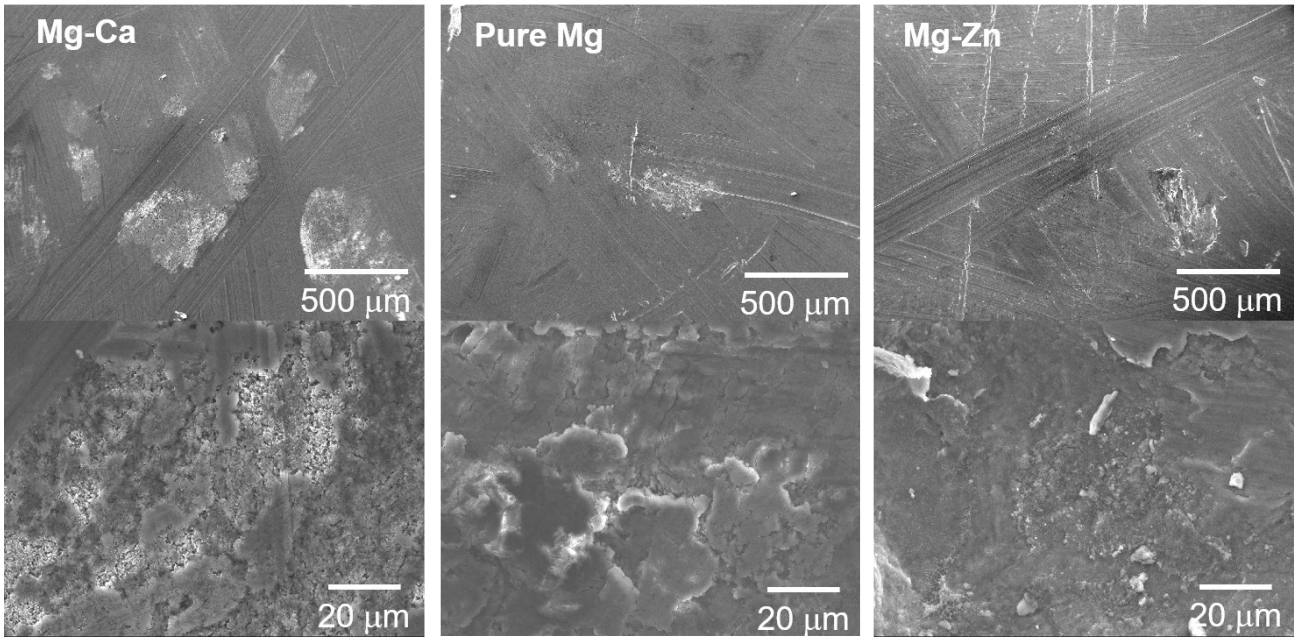

Figure S5. The SEM images of the selected Mg-X alloys after CV cycling. The SEM images clearly indicate that the surface was inhomogeneously utilized irrespective of the alloying elements, however the morphology change upon cycling seems alloying element dependent. Mg-Ca after cycling showed relatively smooth surface while some decomposition products or micro-particles were observed for Mg-Zn.

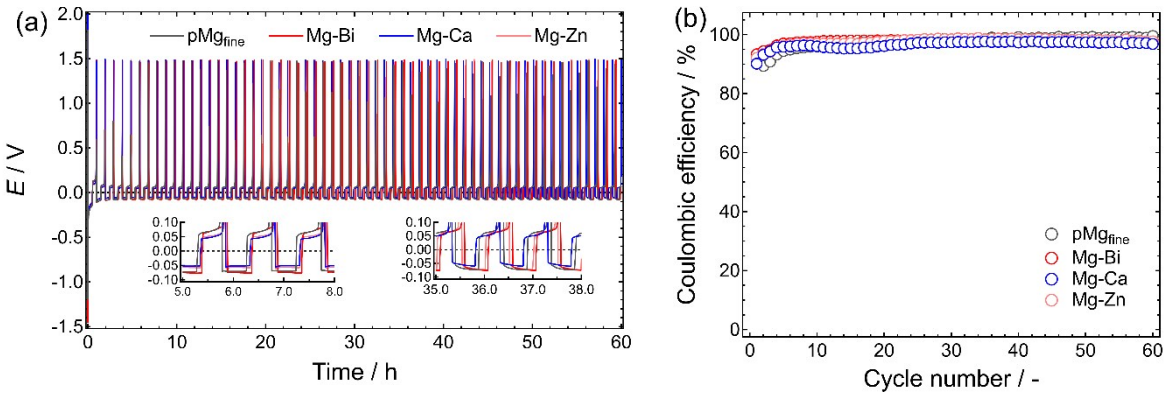

Figure S6. (a) Galvanostatic deposition/dissolution cycling and (b) Coulombic efficiency of [pMg or Mg-X | 0.3 mol dm^{-3} Mg[B(HFIP)$_4$]$_2$/G2 | Cu] cells. The cycling tests were carried out at a current density of 0.5 mA cm^{-2} and 30 °C.

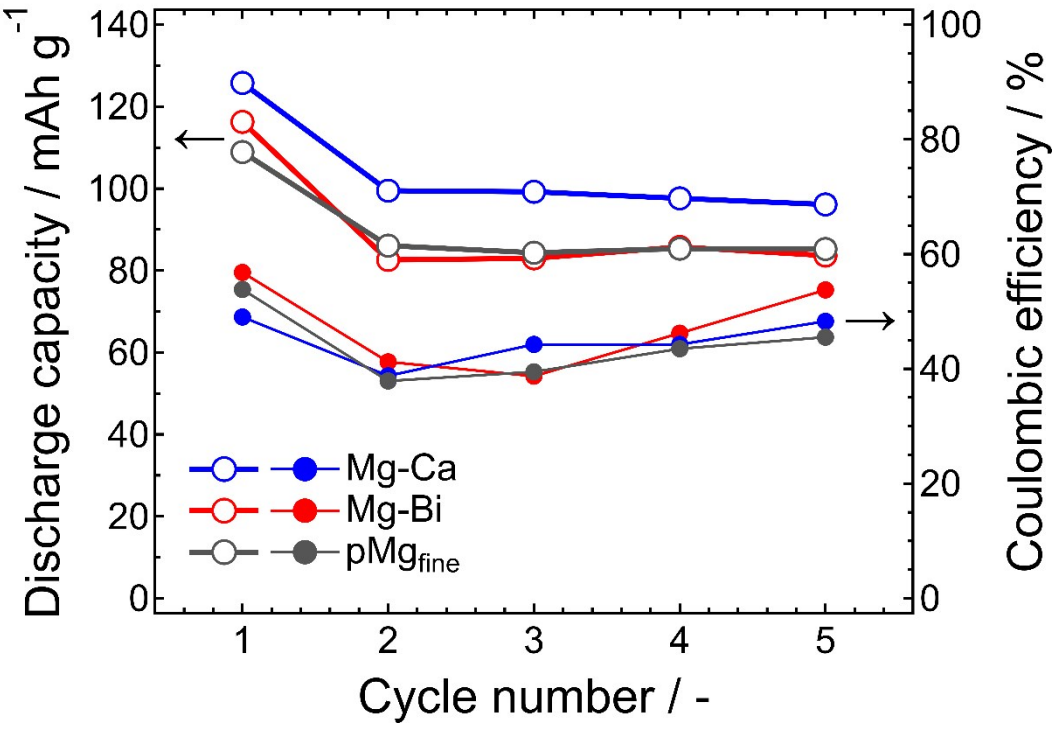

Figure S7. Discharge capacity and corresponding Coulombic efficiency of the [Mg-X |0.3 mol dm^{-3} Mg[B(HFIP)$_4$]$_2$/G2 | $MgMn_2O_4$] cells. A current density of 10.4 mA g^{-1} (1/25 C-rate based on the mass of $MgMn_2O_4$) was applied at 30 °C. Cut-off: +4.0–+0.2 V.

References

1. T. Mandai, *ACS Appl. Mater. Interfaces,* 2020, 12, 39135–39144.

2. T. Mandai, Y. Akita, S. Yagi, M. Egashira, H. Munakata, K. Kanamura, *J. Mater. Chem. A,* 2017, **5**, 3152–3156.

3. K. Ishii, S. Doi, R. Ise, T. Mandai, Y. Oaki, S. Yagi, H. Imai, *J. Alloys Compd*., 2020, **816**, 152556.